applied sciences

MDPI

Article

On the Influence of the Vertical Earthquake Component on Structural Responses of High-Rise Buildings Isolated with Double Friction Pendulum Bearings

Phuong Hoa Hoang [1], Hoang Nam Phan [1,*] and Van Nam Nguyen [2]

[1] Faculty of Road and Bridge Engineering, The University of Danang–University of Science and Technology, Danang 550000, Vietnam; hphoa@dut.udn.vn
[2] Faculty of Civil Engineering, Industrial University of Ho Chi Minh City, Ho Chi Minh City 700000, Vietnam; nguyenvannam@iuh.edu.vn
* Correspondence: phnam@dut.udn.vn

Abstract: The double friction pendulum (DFP) bearing is adapted from the well-known single friction pendulum (SFP) bearing. This type of bearings has been widely used for structural vibration controls. The main advantage of the DFP is its capacity to accommodate larger displacements as compared with the SFP one. This paper aims to assess the effect of the vertical earthquake component on the seismic behaviour of a base-isolated high-rise building. In this respect, the mathematical model of the building subjected to earthquake excitations with an implementation of a DFP bearing system is established. The model presented herein considers earthquake excitations in horizontal (X and Y) and vertical (Z) directions. A series model of two friction elements is presented for the bearing, where the friction load of the bearing surface is governed by a modified Bouc-Wen model, which is dependent on the sliding velocity and the contact pressure. The numerical results of an example of a base-isolated 9-story steel building subjected to near-source and far-field earthquakes show the high effectiveness of the bearing system in reduction of the seismic response of the building, especially in the near-source region, as well as exhibit considerable effectiveness of the vertical earthquake component on the bearing and structural behaviour.

Keywords: seismic isolation; double friction pendulum; high-rise building; vertical earthquake component

Citation: Hoang, P.H.; Phan, H.N.; Nguyen, V.N. On the Influence of the Vertical Earthquake Component on Structural Responses of High-Rise Buildings Isolated with Double Friction Pendulum Bearings. *Appl. Sci.* **2021**, *11*, 3809. https://doi.org/10.3390/app11093809

Academic Editor: Angelo Luongo

Received: 31 March 2021
Accepted: 22 April 2021
Published: 23 April 2021

1. Introduction

Seismic isolation devices have long been applied to control the structural response of buildings and thus to mitigate the extensive damage caused by earthquakes. Structural vibration control techniques under the impact of earthquakes using isolation devices have become one of the core technologies for enhancing the seismic performance of structures in seismic prone areas. These technologies allow a considerable reduction of horizontal seismic actions by shifting the fundamental period of the structures to the range of low spectral acceleration amplitudes [1].

Among different types of isolation systems, the friction pendulum (FP) bearing is one of the most commonly used. This system is designed with special concave surfaces and used to isolate the structure base to the foundation. There are three types of FP bearings, i.e., single friction pendulum (SFP), double friction pendulum (DFP), and triple friction pendulum (TFP), in which the DFP and TFP are new kinds of the SFP with the implementation of sliding surfaces [1,2]. This paper focuses on the DFP, whose main advantage, like TFP, is the capacity to accommodate larger displacements as compared to the former one. The DFP bearing system with articulated sliders, named multiple friction pendulum, as an improved FPS isolator was first analytically and experimentally studied by Tsai et al. [3–5]. Further studies of Constantinou [6] and Fenz and Constantinou [7,8] presented an analytical model to account for unequal curvature radii of the two concave

surfaces and unequal friction coefficients of the two sliding interfaces. Also, in their work, the effects of the height of the articulated slider and the friction in the rotational part of the articulated slider on the lateral force-displacement relation were presented. An advanced DFP bearing model with tri-linear behaviour was later studied by Kim and Yun [9]. The effects of the DFP bearing system with different friction values and restoring properties on a simple bridge are investigated under different earthquakes. These studies have focused on the planar behaviour of the DFB bearing. The effect of the vertical excitation is assumed to be small and is neglected. Besides, recent studies have indicated that the rotational component of earthquakes also affects the overall response of buildings [10]; however, this effect on the DFP bearing has not been investigated so far. Regarding this issue, Faramarz and Montazar [11] studied the effect of the vertical ground acceleration component on the horizontal response of structures isolated with DFP bearings. In which, a mathematical model of the DFP bearing is presented. The model, which represents the force-displacement relationship of the bearing with identical sliding surfaces under bi-directional excitations, is developed based on governing equations of the FP bearing undergoing the unidirectional excitation. The model is simplified by considering equal curvature radii and friction coefficients of the concave surfaces, and hence the sliding velocities on each surface are equal. Recently, Zhou et al. [12] presented a theoretical model of the DFP system under variable vertical loadings and unequal friction coefficients between two sliding surfaces. Both the studies assume a constant friction coefficient of the sliding surface, which is independent of the sliding velocity and the contact pressure. Recently, Bao and Becker [13] developed a three-dimensional DFP bearing model including uplift and impact behaviour; the model facilitates investigations of the extreme behaviour of FP bearing systems.

Experimental studies have also been conducted to investigate the effect of vertical excitation on the horizontal response of buildings. The earlier test was conducted by Fenz and Constantinou [14] for a 6-story building isolated with TP bearings; the authors concluded that the effect of the vertical excitation is minor. Ryan and Dao [15] presented a full-scale shake table experiment of a 5-story frame building isolated with TFP bearings. The finding of the study shows a significant influence of vertical excitation on the horizontal floor accelerations and floor spectra during the test.

Based on the above discussion, this paper focuses on the modelling of base-isolated high-rise buildings implemented with the DFP bearing system, which considers the effect of the vertical earthquake excitation. The aims of the paper are to (i) develop a mathematical model of base-isolated buildings with DFP bearing considering the vertical excitation of earthquakes; the model can accommodate different radii of the concave surfaces, as well as velocity- and surface pressure-dependent friction coefficients; (ii) apply the proposed model to a case study of high-rise steel buildings and investigate the effectiveness of the bearing concerning near-source and far-field earthquakes; and (iii) assess the effect of the vertical excitation on the horizontal response of the building.

2. Modelling of Base-Isolated Buildings with DFP Bearings

2.1. Bidirectional Behaviour

The bidirectional behaviour of the DFP bearing having the schematic and cross-section shown in Figure 1 can be obtained using a series model developed by Fenz and Constantinou [7], as shown in Figure 2. The model in each direction consists of two single friction bearing elements in series, where each element is of a mass m_{bi} ($i = 1$ for the bottom part and $i = 2$ for the top one), a spring with stiffness k_{bi}, a dashpot with damping coefficient c_{bi}, a rigid-plastic friction element with a friction coefficient μ_{ie} that represents the friction behaviour between the bearing surfaces and a gap that represents the displacement limit d_i.

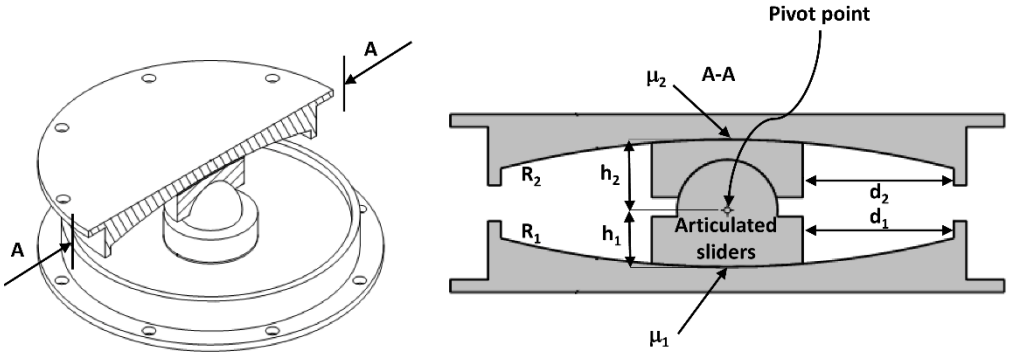

Figure 1. Schematic of the double friction pendulum bearing and its cross-section.

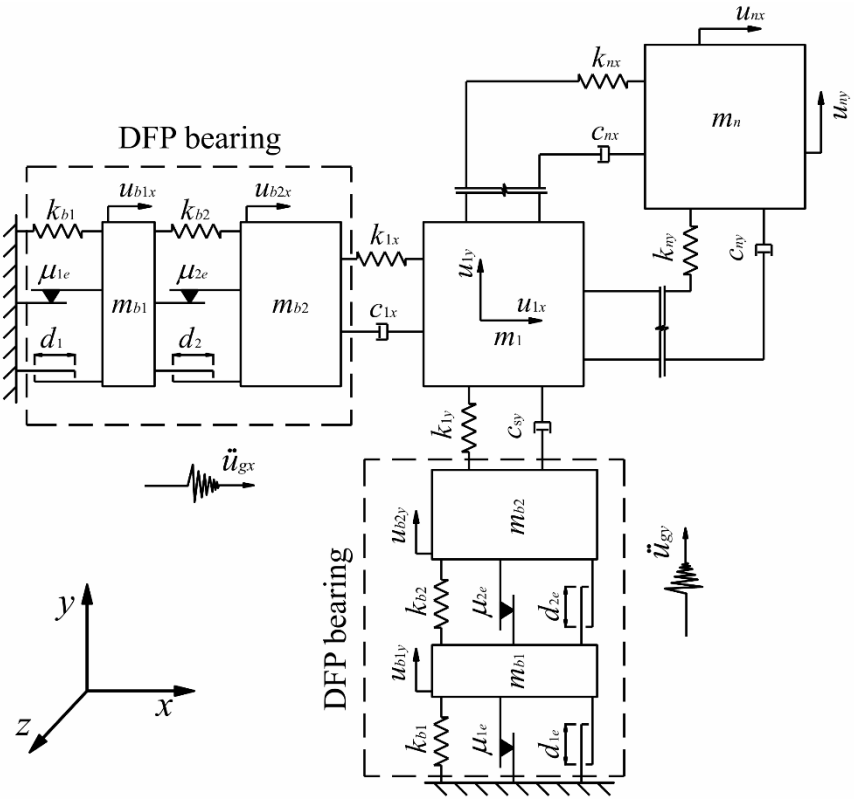

Figure 2. Series model of the DFP bearing and multi-degree of freedom model of the superstructure.

The spring stiffness is calculated based on the effective radius R_{effi} of the spherical surface that represents the linear restoring behaviour (i.e. restoring force), $k_{bi} = W/R_{effi}$, with $R_{effi} = R_i - h_i$, where W is the total weight acting on the bearing, R_i is the radius of curvature i, and h_i is the height from the centre of the pendulum to the surface of curvature i (see Figure 1).

The friction coefficients μ_{ie} have magnitudes depending on the sliding velocity and surface pressure and are determined as

$$\mu_{ie} = \mu_{max} - (\mu_{max} - \mu_{min})e^{-\alpha|\dot{u}_i|}, \quad (1)$$

where μ_{max} and μ_{min} are friction coefficients corresponding to maximum and minimum shear velocities, α is a constant depending on the surface pressure, and $\dot{u}_i = \sqrt{\dot{u}_{ix}^2 + \dot{u}_{iy}^2}$ is the relative radial sliding velocity of element i. In this friction model, the heat flux and temperature increase at each sliding surface are ignored. A more complex model that takes into account the instantaneous velocity and temperature effects on friction at each sliding

surface can be found in the recent work of Sarlis and Constantinou [16]. However, this temperature effect is not very significant; the authors suggested that their complex model can be only used in some special cases.

The model of the superstructure is also presented in Figure 2, in which a multi-degree of freedom linear elastic model is assumed; this is reasonable since the purpose of implementing base isolation is to reduce the earthquake forces on the structure and limit the structural behaviour to an elastic range. As presented in Figure 2, m_i, k_i and c_i are the equivalent lumped mass, stiffness, and damping coefficient of floor i of the building, respectively.

The system of differential equations of motion in each direction includes $(n+2)$ equations (n is the number of floors of the building) can be obtained based on the D'Alembert's principle, given as

$$\begin{cases} m_{b1}\left(\ddot{u}_{b1}+\ddot{u}_g\right)+k_{b1}u_{b1}+F_{f1}+F_{r1}+k_{b2}(u_{b1}-u_{b2})-F_{f2}-F_{r2}=0 \\ m_{b2}\left(\ddot{u}_{b2}+\ddot{u}_g\right)+k_{b2}(u_{b2}-u_{b1})+F_{f2}+F_{r2}+k_1(u_{b2}-u_1)+c_1\left(\dot{u}_{b2}-\dot{u}_1\right)=0 \\ m_1\left(\ddot{u}_1+\ddot{u}_g\right)+k_1(u_1-u_{b2})+c_1\left(\dot{u}_1-\dot{u}_{b2}\right)+k_2(u_1-u_2)+c_2\left(\dot{u}_1-\dot{u}_2\right)=0, \\ \ldots \\ m_n\left(\ddot{u}_n+\ddot{u}_g\right)+k_n(u_n-u_{n-1})+c_n\left(\dot{u}_n-\dot{u}_{n-1}\right)=0 \end{cases} \tag{2}$$

where u_{b1}, u_{b2} and their 1st derivatives are the displacements and velocities of the bottom and top bearing masses, respectively, and $u_1, \ldots, u_n$ and their 1st, 2nd derivatives are the displacements, velocities, and accelerations of the floor masses. The friction force components on the concave surfaces are represented by the Bouc-Wen hysteretic model,

$$\begin{cases} F_{fix}=\mu_{ie}WZ_{ix} \\ F_{fiy}=\mu_{ie}WZ_{iy} \end{cases}, \tag{3}$$

where Z_i is the hysteresis variables describing the variation of the friction coefficients that can be obtained from Equation (4), given as

$$\begin{pmatrix} \dot{Z}_{ix}Y \\ \dot{Z}_{iy}Y \end{pmatrix}=\begin{pmatrix} A\dot{u}_{ix} \\ A\dot{u}_{iy} \end{pmatrix}-\begin{bmatrix} Z_{ix}^2\left(\gamma sign\left(\dot{u}_{ix}Z_{ix}\right)+\beta\right) & Z_{ix}Z_{iy}\left(\gamma sign\left(\dot{u}_{iy}Z_{iy}\right)+\beta\right) \\ Z_{ix}Z_{iy}\left(\gamma sign\left(\dot{u}_{ix}Z_{ix}\right)+\beta\right) & Z_{iy}^2\left(\gamma sign\left(\dot{u}_{iy}Z_{iy}\right)+\beta\right) \end{bmatrix}\begin{pmatrix} \dot{u}_{ix} \\ \dot{u}_{iy} \end{pmatrix}, \tag{4}$$

where the constants in Equation (4) including A, Y, β, γ, and η can be determined followed the work of Constantinou [6].

The impact force is also considered in the model; whose components are determined as

$$\begin{cases} F_{r1x(y)}=k_{r1x(y)}\left(\left|u_{b1x(y)}\right|-d_1\right)sign\left(u_{b1x(y)}\right)H\left(\left|u_{b1x(y)}\right|-d_1\right) \\ F_{r2x(y)}=k_{r2x(y)}\left(\left|u_{b2x(y)}-u_{b1x(y)}\right|-d_2\right)sign(u_{b2x(y)} \\ -u_{b1x(y)})H\left(\left|u_{b2x(y)}-u_{b1x(y)}\right|-d_2\right) \end{cases}, \tag{5}$$

where k_{ri} is the impact stiffness components, $sign$ denotes the signum function and H is the Heaviside step function.

2.2. Considering the Vertical Excitation of Earthquakes

Equation (2) considers the acceleration of ground motion in the two horizontal directions X and Y. In order to include the effect of the vertical component, an additional mass caused by vertical action should be added. The corresponding weight $V(t)$ varying over time is determined as

$$V(t)=W\left(1+\frac{\ddot{u}_{gz}}{g}\right), \tag{6}$$

where $\ddot{u}_{gz}$ is the vertical acceleration component of the ground motion; g is the acceleration of gravity, and W is the total weight above the bearing.

The stiffness of springs from the above series model is recalculated as

$$\begin{cases} k_{bz1} = \frac{V(t)}{R_{eff1}} \\ k_{bz2} = \frac{V(t)}{R_{eff2}} \end{cases}. \quad (7)$$

Similarly, Equation (3) is rewritten considering the effect of the vertical component of the ground motion,

$$\begin{cases} F_{fz1} = \mu_1 V(t) Z_1 \\ F_{fz2} = \mu_2 V(t) Z_2 \end{cases}. \quad (8)$$

As a result, a system of differential equations of motion of the structural system under the impact of the ground acceleration of earthquakes in 3 directions X, Y, and Z is obtained as

$$\begin{cases} m_{b1}\left(\ddot{u}_{b1} + \ddot{u}_g\right) + k_{bz1}u_{b1} + F_{fz1} + F_{r1} + k_{bz2}(u_{b1} - u_{b2}) - F_{fz2} - F_{r2} = 0 \\ m_{b2}\left(\ddot{u}_{b2} + \ddot{u}_g\right) + k_{bz2}(u_{b2} - u_{b1}) + F_{fz2} + F_{r2} + k_1(u_{b2} - u_1) + c_1\left(\dot{u}_{b2} - \dot{u}_1\right) = 0 \\ m_1\left(\ddot{u}_1 + \ddot{u}_g\right) + k_1(u_1 - u_{b2}) + c_1\left(\dot{u}_1 - \dot{u}_{b2}\right) + k_2(u_1 - u_2) + c_2\left(\dot{u}_1 - \dot{u}_2\right) = 0 \\ \ldots \\ m_n\left(\ddot{u}_n + \ddot{u}_g\right) + k_n(u_n - u_{n-1}) + c_n\left(\dot{u}_n - \dot{u}_{n-1}\right) = 0 \end{cases} \quad (9)$$

The motion equations can be solved by the fourth-order Runge-Kutta numerical method using the ode15s solver in the MATLAB software [17].

3. Description of Case Study and Ground Motion Inputs

The seismic response of a 9-storey steel building with and without DFP bearings is investigated in this study. As mentioned before, a linear elastic model for the building can be assumed in this case since the aim of the isolation system is to limit the building behaviour in the elastic range. Moreover, the emphasis of the paper is on the behaviour of the bearing rather than the building. It has also been seen that the stiffness of the floors is considerably higher than the overall stiffness of the storey due to the columns. Thus, each floor diaphragm constituted by slabs and beams can be assumed to be a rigid diaphragm. As a result, a shear building model is presented, and the torsion effect is ignored in this study.

Figure 3 shows spring-mass models of the building with and without DFP bearings. In these models, the soil-structure interaction (SSI) effect is neglected. However, many studies have indicated that a system of the steel building-foundation should be taken into account, especially ones subjected to near-source earthquakes [18]. An input, the values of mass and stiffness of each floor are assumed to be the same, given as: m_i = 0.0714 kNs^2/mm and k_i = 100 kN/mm. These values are approximately selected according to the full-scale steel building model from the experimental test by Ryan et al. [15]. The damping ratio (ξ) is chosen as 2.5%, resulting in the fundamental period of the structure T_1 = 1.016 s. Concerning the bearing characteristics, the following values are selected:

- effective radii $R_{eff1} = R_{eff2}$ = 1968 mm,
- displacement limits $d_1 = d_2$ = 250 mm,
- friction coefficients μ_1 = 0.02–0.06, μ_2 = 0.06–0.1, $\alpha = 0.02$,
- and constants in Equation (4) are selected based on the work of Constantinou [6], i.e., $A = 1$, $Y = 0.25$, $\beta = 0.1$, $\gamma = 0.9$, and $\eta = 2$.

The input ground motions of the Northridge-01 event are obtained from the PEER NGA-West2 database [19]. These records are selected from two stations Rinaldi Receiving and LA-Obregon Park with epicentral distances of 6.5 and 37.36 km, respectively. The selection aims to distinguish two different cases of the ground motion characteristic, i.e., near-source and far-field. The site to fault distance for the near-source ground motion is commonly defined to be less than 10 km [20]. The detail of the selected ground motions is

illustrated in Table 1, whereas their time history data of the two horizontal components is shown in Figure 4, along with 5%-damping elastic response spectra.

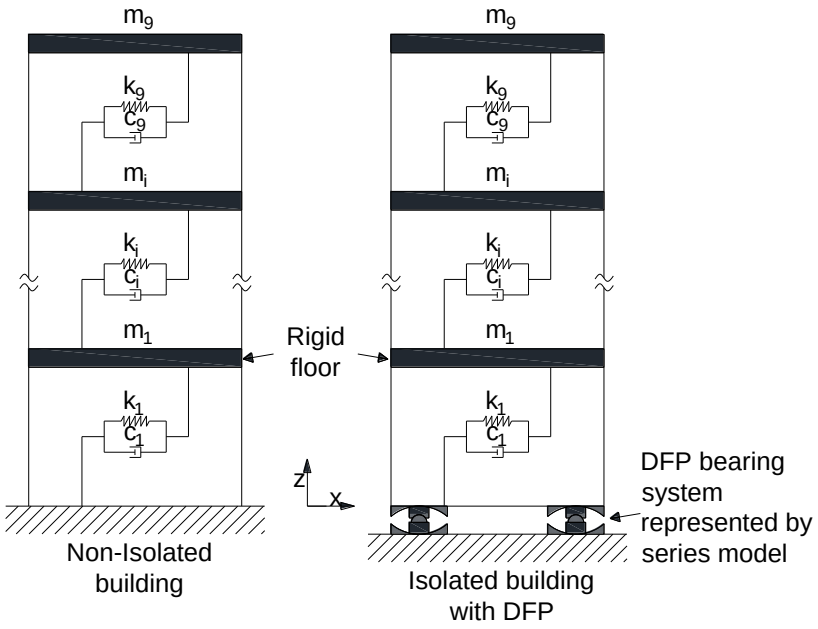

Figure 3. Lumped mass model of the examined 9-storey steel building with and without DFP bearing (XZ plane).

Table 1. The characteristics of the ground motions.

N.	Event	Station	M_W	R_{rup} (km)	Soil Type	PGA (g)		
						X	Y	Z
Record 1	Northridge-01 (1994)	Rinaldi Receiving	6.69	6.50	D	0.874	0.472	0.958
Record 2	Northridge-01 (1994)	LA-Obregon Park	6.69	37.36	D	0.568	0.514	0.217

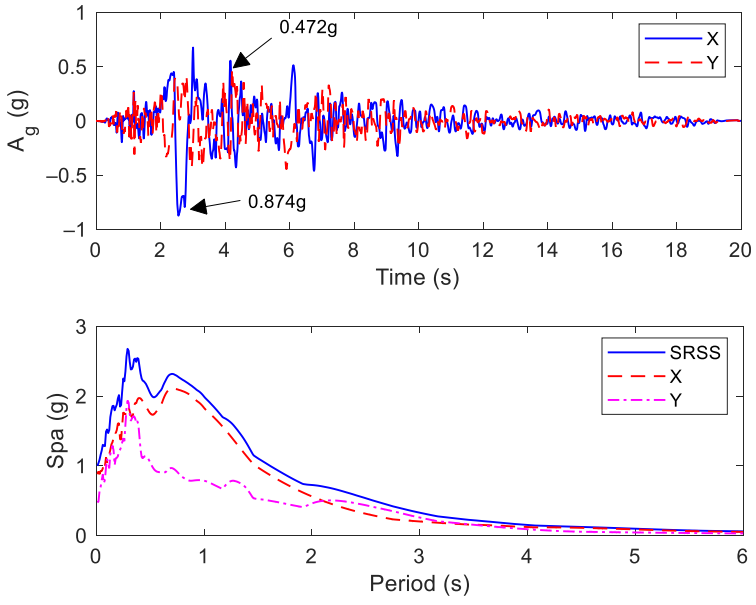

(**a**)

Figure 4. *Cont.*

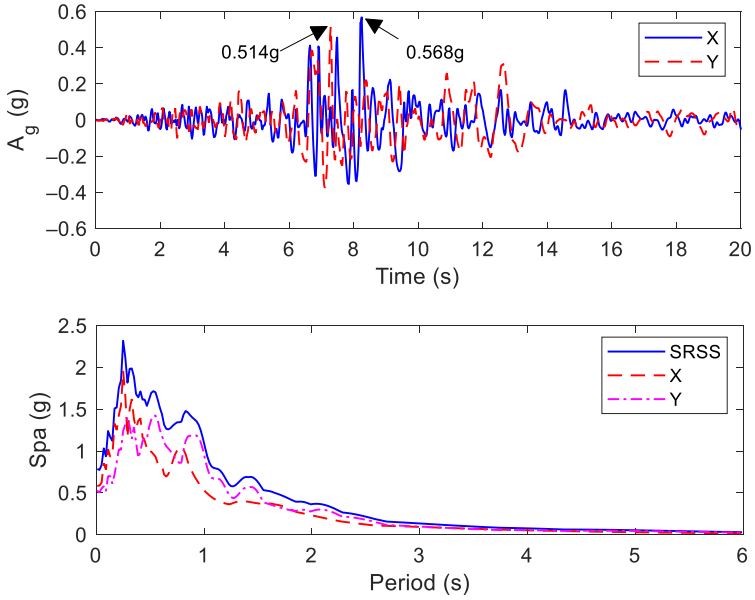

(**b**)

Figure 4. Acceleration time history data and response spectra of the selected ground motions: (**a**) Rinaldi Receiving station and (**b**) LA-Obregon Park station.

4. Analysis Results

The equations of motion of the fixed base and isolated base buildings are established based on the input parameters presented previously. The set of ordinary differential equations is solved by the fourth-order Runge-Kutta numerical method using the ode15s function in the MATLAB software. The numerical results in terms of time-history data of the absolute acceleration and shear force for the non-isolated and isolated cases of the building subjected to three components of the excitation are shown in Figures 5–8. The peak responses of the two cases are summarized in Table 2, where the responses of the building considering only two horizontal components are also added for the comparison.

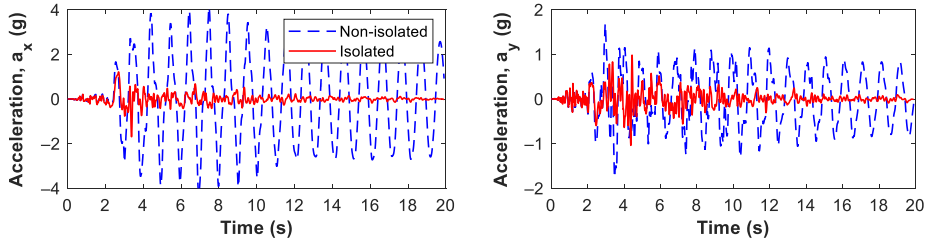

(**a**) (**b**)

Figure 5. Time history of roof absolute acceleration of the building subjected to Record 1: (**a**) X-response and (**b**) Y-response.

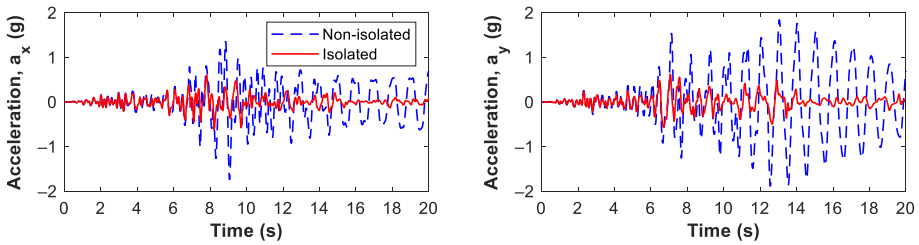

(**a**) (**b**)

Figure 6. Time history of roof absolute acceleration of the building subjected to Record 2: (**a**) X-response and (**b**) Y-response.

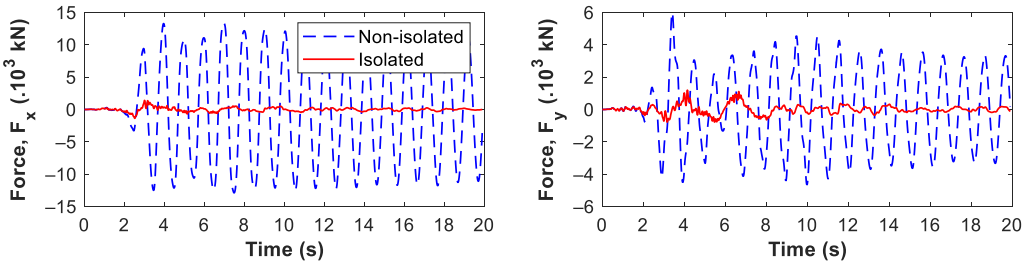

(**a**) (**b**)

Figure 7. Time history of the 1st-floor shear force of the building subjected to Record 1: (**a**) X-response and (**b**) Y-response.

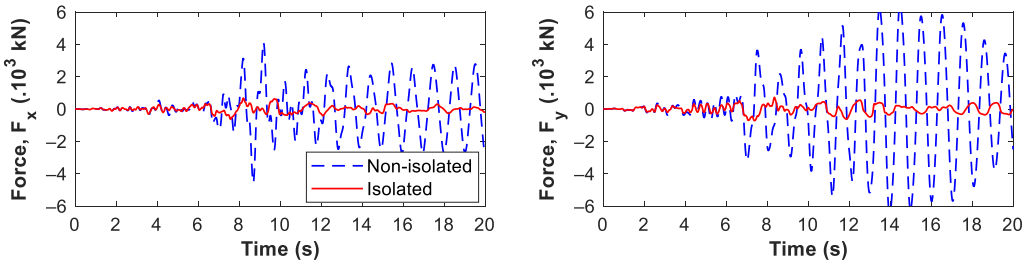

(**a**) (**b**)

Figure 8. Time history of the 1st-floor shear force of the building subjected to Record 2: (**a**) X-response and (**b**) Y-response.

Table 2. Peak seismic response of the building.

Ground Motion	Response	Non-Isolated	Isolated (XY)	Per. of Reduc. (%)	Isolated (XYZ)	Per. of Reduc. (%)
Record 1 (near-source)	Roof accel.-X (g)	4.285	1.038	76	1.690	61
	Roof accel.-Y (g)	1.760	0.608	65	1.038	41
	1st-floor shear-X (kN)	1.331×10^4	1.033×10^3	92	1.409×10^3	89
	1st-floor shear-Y (kN)	5.988×10^3	9.332×10^2	84	1.197×10^3	80
Record 2 (far-field)	Roof accel.-X (g)	1.741	0.582	67	0.617	65
	Roof accel.-Y (g)	1.890	0.610	68	0.623	67
	1st-floor shear-X (kN)	4.546×10^3	6.017×10^2	87	6.788×10^2	85
	1st-floor shear-Y (kN)	6.564×10^3	6.996×10^2	89	7.255×10^2	89

The results show the high effectiveness of the isolation system in the reduction of the seismic response of the building. For example, in most cases, a reduction of about 60% in terms of the roof acceleration is recorded when the DFP bearing system is implemented, and that figure for the 1st-floor shear force is about 80%.

The comparison of the peak responses when the isolated building is subjected to only two horizontal components (XY) and three components (XYZ) is also shown in Table 2. It can be seen that there is a considerable increase in terms of the acceleration and shear force when the vertical excitation is included in the model, resulting in the effectiveness of the bearing decreases. The increase of the seismic response compared with the bi-directional case is more significant in the case of near-source record; in detail, the difference of the

percentage of reduction between the two cases is about 15% for the X-response of the acceleration and 24% for the Y-response. The comparative results demonstrate the necessity of considering the impact of the vertical excitation on the isolated building.

The hysteresis loops (i.e., the shear force-displacement relationship of the bearing) under bi- and tri-directional excitations of the two earthquakes are shown in Figure 9. In these figures, the shear forces are normalized to the vertical weight of the superstructure. This again exhibits the considerable effect of the vertical impact on the behaviour of the bearing subjected to the near-source earthquake Figure 9a,b. For the far-field record, the behaviours of the two cases are almost the same Figure 9a,b.

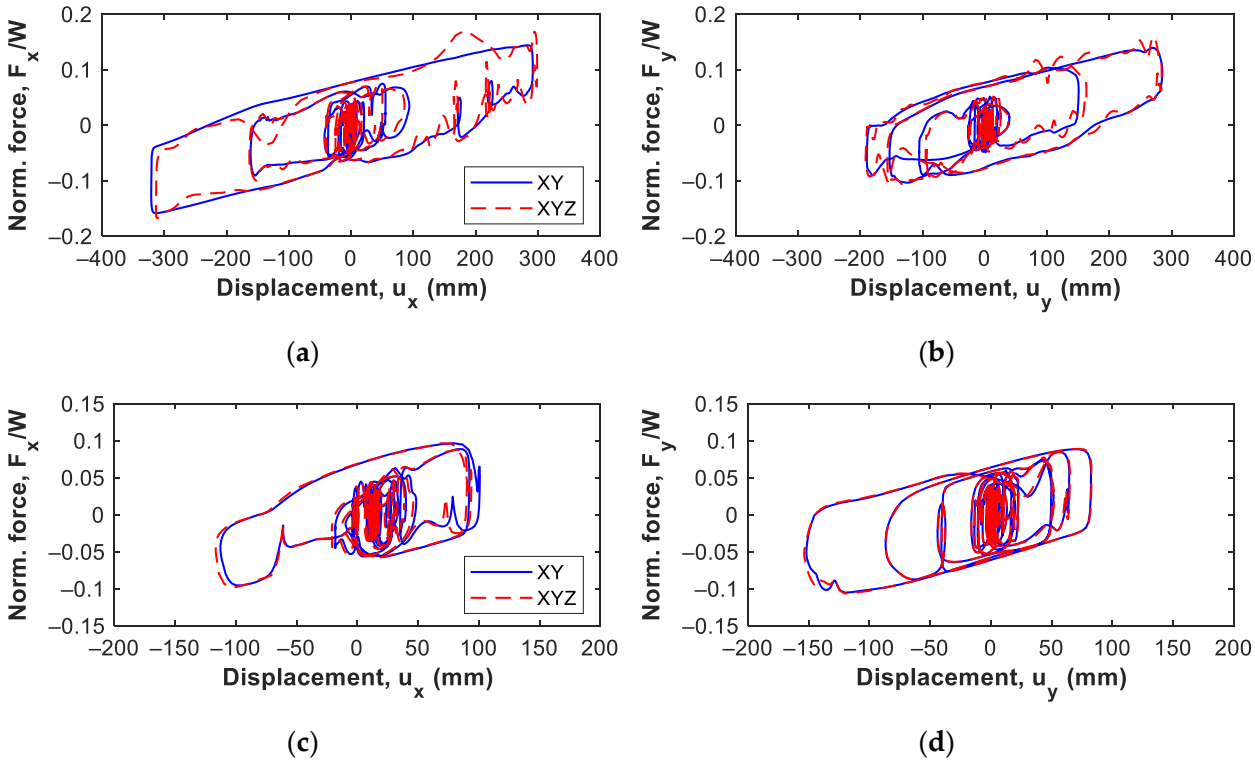

Figure 9. Hysteresis loops under bi- and tri-directional excitations: (**a**,**b**) X- and Y-response of the near-source earthquake and (**c**,**d**) X- and Y-response of the far-field earthquake.

The seismic responses of each floor are also obtained from the analyses. Figures 10 and 11 show the effect of the vertical component of excitation along the height of the building, as compared to the bi-directional and fixed cases. The effects are quantified in terms of the absolute acceleration and shear force of each floor. In the case of a near-source earthquake, a remarkable increase of the response is obtained from figures; this demonstrates the significant effect of the vertical excitation of the earthquakes on the total response of structures, especially high-rise buildings. The effect of tri-directional excitation when the isolated building subjected to the far-field earthquake is limited. A slight increase of the peak acceleration response is recognized in most of the floors, except the second to the fourth floor, the response considerably increases as compared with the bi-directional case Figure 10b. Similar observation can be found in the shear force response of each floor (Figure 11).

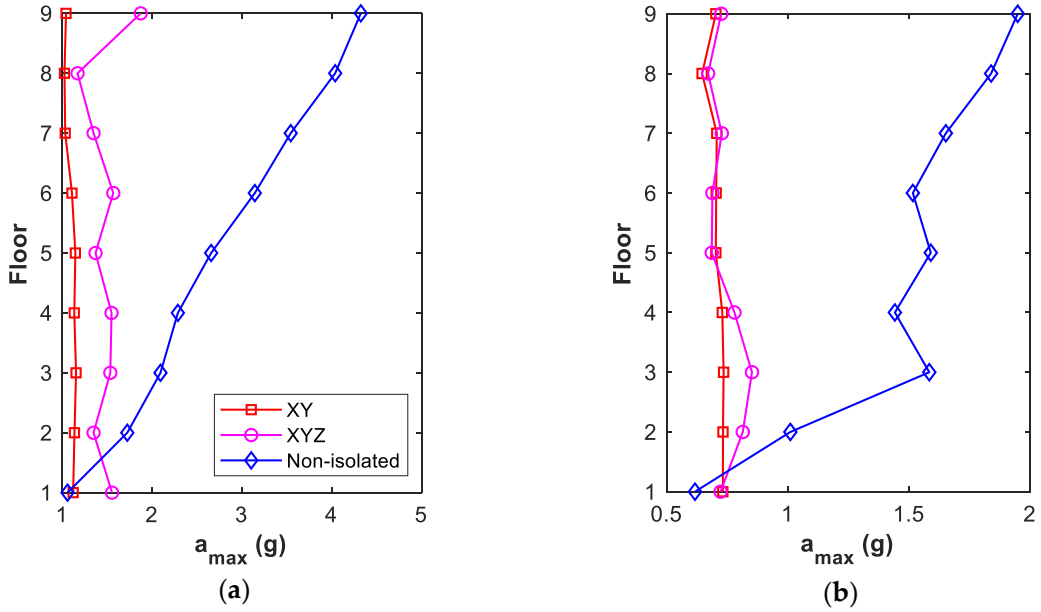

Figure 10. Peak acceleration on each floor under bi- and tri-directional and fixed-base cases: (**a**) the near-source record and (**b**) the far-field record.

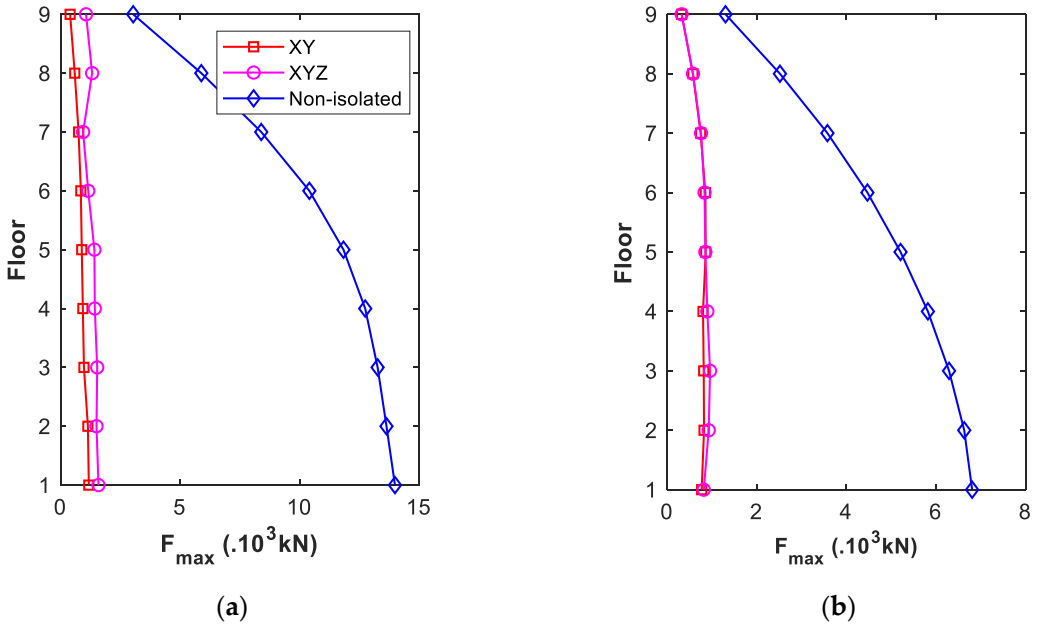

Figure 11. Peak shear force on each floor under bi- and tri-directional and fixed-base cases: (**a**) the near-source record and (**b**) the far-field record.

The movements of the slider on the sliding surfaces of the bearing during the earthquakes are also plotted in Figure 12. Since the impact force has been considered in the analytical model of the bearing, the sliders move on the concave surfaces within their displacement limits. The movement of the slider on each concave surface is different. For example, in Figure 12a concerning the near-source record, the slider reaches the maximum displacement and impacts the retainer ring of concave surface 1, while the movement of the slider on surface 2 is rather small.

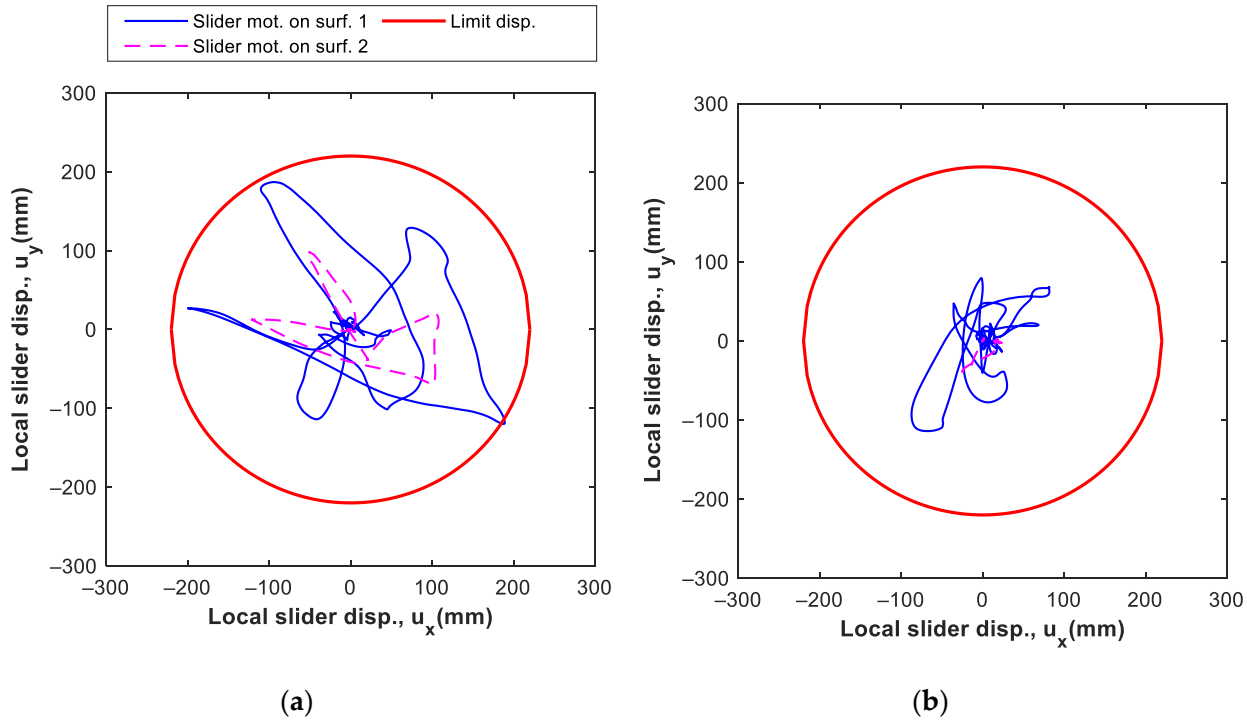

Figure 12. The movements of the pendulum on the sliding surfaces: (**a**) the near-source earthquake and (**b**) the far-field earthquake.

5. Conclusions

A mathematical model of isolated buildings based on DFP bearings is presented in this paper. The bearings are simulated through a series model considering a velocity- and pressure-dependent friction model and the vertical component of ground motions. The analysis results are obtained for a 9-storey steel building subjected to near-source and far-field earthquakes. Comparative results between non-isolated and isolated cases of the building demonstrate the high effectiveness of the DFP bearings in the reduction of the seismic response of high-rise buildings. As a result, the seismic responses of the building are significantly reduced. In most cases, the roof acceleration decreases about 60% and the first-floor shear force decreases about 80% as compared to the fixed base condition.

The findings of the study also show the significant effect of the vertical component of the earthquake on the overall response of the building, especially in the case of the near-source earthquake. In detail, the response of the building considerably increases in the tri-directional case as compared with the bi-directional one. For example, the difference in the percentage of reduction between the two cases is about 15% for the X-response of the acceleration and 24% for the Y-response.

Author Contributions: Conceptualization, P.H.H. and V.N.N.; methodology, P.H.H. and V.N.N.; software, H.N.P. and V.N.N.; formal analysis, H.N.P. and V.N.N.; investigation, H.N.P. and V.N.N.; writing—original draft preparation, P.H.H., H.N.P. and V.N.N.; writing—review and editing, P.H.H., H.N.P. and V.N.N. All authors have read and agreed to the published version of the manuscript.

Funding: This research is funded by Funds for Science and Technology Development of the University of Danang under project number B2019-DN02-55.

Institutional Review Board Statement: Not applicable.

Informed Consent Statement: Not applicable.

Data Availability Statement: The data used to support the findings of this study are available from the corresponding author upon request.

Conflicts of Interest: The authors declare no conflict of interest.

References

1. Buckle, I.G.; Mayes, R.L. Seismic Isolation: History, Application, and Performance—A World View. *Earthq. Spectra* **1990**, *6*, 161–201. [CrossRef]
2. Phan, H.N.; Paolacci, F.; Corritore, D.; Akbas, B.; Uckan, E.; Shen, J.J. Seismic vulnerability mitigation of liquefied gas tanks using concave sliding bearings. *Bull. Earthq. Eng.* **2016**, *14*, 3283–3299. [CrossRef]
3. Tsai, C.S.; Chiang, T.; Chen, B. Seismic behavior of MFPS isolated structure under near-fault sources and strong ground motions with long predominant periods. In Proceedings of the ASME 2003 Pressure Vessels and Piping Conference, Cleveland, OH, USA, 20–24 July 2003; pp. 73–79.
4. Tsai, C.S.; Cheng, T.; Chen, B.J. Experimental evaluation of piecewise exact solution for predicting seismic responses of spherical sliding type isolated structures. *Earthq. Eng. Struct. Dyn.* **2005**, *34*, 1027–1046. [CrossRef]
5. Tsai, C.S.; Chen, W.S.; Chiang, T.C.; Chen, B.J. Component and shaking table tests for full-scale multiple friction pendulum system. *Earthq. Eng. Struct. Dyn.* **2006**, *35*, 1653–1675. [CrossRef]
6. Constantinou, M.C. *Friction Pendulum Double Concave Bearing*; Technical Report; University at Buffalo, State University of New York: Buffalo, NY, USA, 2004.
7. Fenz, D.M.; Constantinou, M.C. Behaviour of the double concave Friction Pendulum bearing. *Earthq. Eng. Struct. Dyn.* **2006**, *35*, 1403–1424. [CrossRef]
8. Fenz, D.M.; Constantinou, M.C. Spherical sliding isolation bearings with adaptive behavior: Theory. *Earthq. Eng. Struct. Dyn.* **2008**, *37*, 163–183. [CrossRef]
9. Kim, Y.S.; Yun, C.B. Seismic response characteristics of bridges using double concave friction pendulum bearings with tri-linear behaviour. *Eng. Struct.* **2007**, *29*, 3082–3093. [CrossRef]
10. Pnevmatikos, N.; Konstandakopoulou, F.; Papagiannopoulos, G.; Hatzigeorgiou, G.; Papavasileiou, G. Influence of Earthquake Rotational Components on the Seismic Safety of Steel Structures. *Vibration* **2020**, *3*, 42–50. [CrossRef]
11. Faramarz, K.; Montazar, R. Seismic response of double concave friction pendulum base-isolated structures considering vertical component of earthquake. *Adv. Struct. Eng.* **2010**, *13*, 1–13. [CrossRef]
12. Zhou, F.; Xiang, W.; Ye, K.; Zhu, H. Theoretical study of the double concave friction pendulum system under variable vertical loading. *Adv. Struct. Eng.* **2019**, *22*, 1998–2005. [CrossRef]
13. Bao, Y.; Becker, T. Three-dimensional double friction pendulum bearing model including uplift and impact behavior: Formulation and numerical example. *Eng. Struct.* **2019**, *199*, 109579. [CrossRef]
14. Fenz, D.M.; Constantinou, M.C. *Development, Implementation and Verification of Dynamic Analysis Models for Multi-Spherical Sliding Bearings*; Technical Report MCEER-08-0018; Multidisciplinary Center for Earthquake Engineering Research, State Univeraity of New York at Buffalo: Buffalo, NY, USA, 2008.
15. Ryan, K.L.; Dao, N.D. Influence of Vertical Ground Shaking on Horizontal Response of Seismically Isolated Buildings with Friction Bearings. *J. Struct. Eng.* **2015**, *142*, 04015089. [CrossRef]
16. Sarlis, A.A.; Constantinou, M.C. A model of triple friction pendulum bearing for general geometric and frictional parameters. *Earthq. Eng. Struct. Dyn.* **2016**, *45*, 1837–1853. [CrossRef]
17. The MathWorks, Inc. 2019. Documentation. Available online: https://www.mathworks.com/help/matlab (accessed on 4 January 2021).
18. Katsimpini, P.; Konstandakopoulou, F.; Papagiannopoulos, G.; Pnevmatikos, N.; Hatzigeorgiou, G. Seismic Performance of Steel Structure-Foundation Systems Designed According to Eurocode 8 Provisions: The Case of Near-Fault Seismic Motions. *Buildings* **2020**, *10*, 63. [CrossRef]
19. Pacific Earthquake Engineering Research Center (PEER) Ground Motion Database. Available online: http://ngawest2.berkeley.edu (accessed on 18 January 2021).
20. Gorai, S.; Maity, D. Numerical investigation on seismic behaviour of aged concrete gravity dams to near source and far source ground motions. *Nat. Hazards* **2021**, *105*, 943–966. [CrossRef]